Drug Design, Development and Therapy

Dovepress
Taylor & Francis Group

Open Access Full Text Article

CLINICAL TRIAL REPORT

Exploring the Population Pharmacokinetic and Pharmacogenetics Characteristics of Flurbiprofen Isomers in Selective Joint Replacement Patients with Postoperative Pain

Han Yao[1,*], Xingxian Luo[2,*], Jinjie Yuan[3], Hong Zhang[1], Haiyan An[1], Yi Feng[1]

[1]Department of Anesthesiology, Peking University People's Hospital, Beijing, People's Republic of China; [2]Department of Pharmacy, Peking University People's Hospital, Beijing, People's Republic of China; [3]National Institution of Drug Clinical Trial, the First Affiliated Hospital of Soochow University, Suzhou, People's Republic of China

*These authors contributed equally to this work

Correspondence: Yi Feng, Department of Anesthesiology, Peking University People's Hospital, Beijing, 100044, People's Republic of China, Email doctor_yifeng@sina.com

Purpose: Flurbiprofen plays a critical role in clinical pain management. This study aims to elucidate the population pharmacokinetic (PPK) profiles of flurbiprofen's enantiomers, R(-) and S(+)-flurbiprofen in human subjects, following intravenous administration, while investigating the influence of clinical covariates.

Patients and Methods: PPK modeling of flurbiprofen isomers was based on a prospective study that included a total of 67 patients, each of whom had plasma and cerebrospinal fluid (CSF) samples collected at various time points within 5–50 min. Nonlinear mixed effects modeling was performed using Phoenix NLME. The final PPK model was validated using both Bootstrap and visual prediction checks. Modeling was used to assess the effect of demographic, biological, and pharmacogenetic (12 SNPs relatived to CYP2C9, ABCB1, PXR, POR and UGT1A9) covariates on clearance (CL) and apparent volume of distribution (V_d) for R(-) and S(+)-flurbiprofen.

Results: A two-compartment model best fit the data. All patients were homozygous for the wild-type CYP2C9 allele. Plasma CL of S (+)-flurbiprofen was significantly influenced by ABCB1 (rs1045642) polymorphisms. For R(-)-flurbiprofen, body surface area (BSA) were related to V_d while POR (rs1057868) polymorphisms were associated with CL. The V_d for both R(-)- and S(+)-flurbiprofen was found to be larger in CSF compared to plasma. Specifically, the final model estimated the Vd of R(-)-flurbiprofen (CSF 79.1 L VS plasma 17.1 L) and S(+)-flurbiprofen (CSF 32.6 L VS plasma 25.6 L), and the CL of R(-)-flurbiprofen (CSF 0.45L·h^{-1} VS plasma 11.8L·h^{-1} and S(+)-flurbiprofen (0.39 L·h^{-1} VS plasma 16.7 L·h^{-1}), respectively.

Conclusion: Key covariates of S (+)-flurbiprofen was ABCB1 gene polymorphisms and R-flurbiprofen was POR gene polymorphisms and BSA. The findings may provide support for future dose optimization and the development of novel therapeutic approaches.

Keywords: flurbiprofen, enantiomers, cerebrospinal fluid, population pharmacokinetic, gene polymorphsim

Introduction

Non-steroidal anti-inflammatory drugs (NSAIDs), as a widely used class of analgesic agents, play a significant role in perioperative pain management.[1,2] By inhibiting cyclooxygenase (COX) activity and reducing prostaglandin synthesis, they exert analgesic, anti-inflammatory, and antipyretic effects.[3] Among them, flurbiprofen axetil, an intravenous NSAID, has become one of the most commonly used perioperative analgesics in many countries due to its unique drug delivery system and high analgesic efficacy.[4,5] Specifically, flurbiprofen axetil is released from lipid microspheres and rapidly hydrolyzed by carboxylesterase into its active metabolite flurbiprofen, thereby mediating its pharmacological effects.[6]

Received: 25 May 2025
Accepted: 26 September 2025
Published: 9 October 2025

Furbiprofen undergoes extensive metabolism primarily via hydroxylation mediated by cytochrome P450 (CYP) 2C9 and glucuronidation catalyzed by UDP-glucuronosyltransferases (UGT) 2B7 and UGT1A9.[7,8] Following intravenous administration, flurbiprofen axetil is completely hydrolyzed to flurbiprofen within 5 minutes, with peak plasma concentrations of flurbiprofen achieved 6–7 minutes post-administration and a plasma elimination half-life of 5.8 hours. Approximately 50% of the drug is excreted in urine within 24 hours. The pharmacokinetics of flurbiprofen exhibit significant interindividual variability, which may be closely related to CYP2C9 genetic polymorphisms, height, body weight, and other factors.[7–10]

In recent years, the enantiomers of flurbiprofen, namely the S(+) and R(-)-form, have garnered significant attention. Studies have revealed that the anti-inflammatory efficacy of S(+)-flurbiprofen is 100-fold greater than that of R-flurbiprofen.[11] Consequently, the development of S(+)-flurbiprofen may present a superior therapeutic option for the treatment of inflammatory diseases.[12,13] R-flurbiprofen has been demonstrated to exhibit amyloid-lowering effects, positioning it as a potential therapeutic agent for Alzheimer's disease.[14]

The characterization of flurbiprofen's distribution into the cerebrospinal fluid (CSF) is clinically significant as it is directly relevant to its central analgesic effects and the incidence of centrally-mediated adverse drug reactions. Interestingly, previous studies have revealed significant distribution differences between S(+)- and R(-)-flurbiprofen in plasma and CSF, with the S-enantiomer showing markedly higher transport ratios from plasma to CSF compared to the R-enantiomer.[15] This distribution disparity may be attributed to variations in blood-brain barrier permeability, protein binding rates, and metabolic pathways between the two enantiomers. Despite these recognized differences, a systematic investigation into the critical factors governing the stereoselective disposition of flurbiprofen enantiomers, particularly through the development of a population pharmacokinetic model, is still lacking. Understanding the pharmacokinetic profiles of flurbiprofen enantiomers in human plasma and CSF will not only help optimize perioperative analgesic strategies, but also provide clinically important insights for developing novel enantiomer-based therapies.

Therefore, to address this unmet need and pave the way for precision medicine with flurbiprofen axetil, this study was designed to systematically characterize the stereoselective pharmacokinetics of S(+)- and R(-)-flurbiprofen in a surgical patient population. By integrating genetic polymorphisms and demographic factors, we systematically evaluate their impact on enantiomer pharmacokinetics. These models will facilitate the understanding of the mechanism of flurbiprofen while providing important support for drug development and personalized therapeutic strategies.

Materials and Methods

Patients and Study Design

Inclusion criteria: Patients aged 18–85 years, scheduled for elective unilateral joint replacement surgery, who are to receive spinal anesthesia and classified as ASA physical status I–III. Exclusion criteria: Patients with asthma, liver or kidney dysfunction, peptic ulcer, or allergy to non-steroidal anti-inflammatory drugs; those who have taken non-steroidal anti-inflammatory drugs or CYP2C9 inhibitors (such as cimetidine, amiodarone, fluconazole, ketoconazole, and voriconazole) and inducers (such as rifampicin and barbiturates) within two weeks prior to surgery; and patients with plasma total protein and albumin levels below the normal range.

Exclusion criteria: (1) Failure of subarachnoid puncture, resulting in inability to collect CSF; (2) Inability to collect CSF or venous blood samples in a timely manner according to the grouping; (3) Difficulty in collecting CSF samples due to CSF outflow issues; (4) Blood contamination in the collected CSF samples; or (5) Hemolysis in plasma samples obtained through venous blood centrifugation. This study was approved by Ethical Review Committee of Peking University People's Hospital (#2019PHB169-01) and registered as a clinical trial (ClinicalTrials.gov Identifier: NCT04128410). All participants provided written informed consent prior to enrollment, and the study was conducted in accordance with the Declaration of Helsinki.

After the patient enters the operating room, an intravenous access was established in the upper limb. Then, electrocardiogram (ECG), blood pressure (BP), and pulse oxygen saturation (SpO2) were monitored. Prior to subarachnoid anesthesia, all patients receive an intravenous injection of 1 mg midazolam, followed by an intravenous injection of 100 mg flurbiprofen ester (FEX, 5050 E, Beijing Tide Pharmaceutical Co., Ltd., Beijing, China) at a rate of 2 mL/min

based on the manufacturer's instruction. Based on the pharmacokinetic profile of flurbiprofen axetil, where complete hydrolysis to the active metabolite occurs within 5 minutes and peak plasma concentrations are achieved at 6–7 minutes post-dose, we implemented an intensive sampling strategy with blood and CSF collections every 5 minutes until the 50-minute mark to fully characterize the critical distribution phase and early elimination kinetics of both enantiomers. The venous blood sample collection site was the contralateral upper limb's median cubital vein. Patients were randomly divided into 10 groups using a block randomization method, with 7 patients in each group, and samples were taken at different time points: pre-administration as T0; the group sampled 5 minutes post-administration as T5; the group sampled 10 minutes post-administration as T10; and so on, until T50 at 50 minutes.

A senior anesthesiologist performed the L2-3 or L3-4 interspace puncture for subarachnoid anesthesia, collecting blood and CSF samples before injecting the local anesthetic into the subarachnoid space. To account for potential clinical delays, preparations for the subarachnoid puncture were made 10 minutes prior to the scheduled sampling. After successful subarachnoid puncture, 1 mL of clear CSF was collected using a 2 mL sterile syringe. Simultaneously, a circulating nurse assisted in collecting 2 mL of venous blood into a heparinized tube. Subsequently, 15–20 mg of ropivacaine was injected into the subarachnoid space for spinal anesthesia, based on the surgery and patient condition.

Pharmacokinetic Study

Stereospecific Determination of Flurbiprofen in Plasma and Cerebrospinal Fluid

The negative ion mode electrospray ionization liquid chromatography-tandem mass spectrometry (LC-MS/MS) was used to determine the two enantiomers of flurbiprofen, R(-) and S(+), in the plasma and CSF of patients based on the previous literature.[14] The internal standard (IS), R(-), and S(+) flurbiprofen were separated using a CHIRALPAK-IG3 column (250 mm × 4.6 mm) at 25°C, with acetonitrile/ammonium formate as the mobile phase in a 90:10 (v/v) ratio at a flow rate of 0.4 mL/min. Quantification was performed in multiple reaction monitoring mode, with IS transitions of m/z 253.1→209.1, and R(-) and S(+) flurbiprofen transitions of m/z 243.1→199.1.

The lower limits of quantification for plasma and CSF were 0.1 μg/mL and 1 ng/mL, respectively. The calibration curves for plasma and CSF samples were linear from 0.1–10 μg/mL and 1–100 ng/mL, respectively. The retention times for IS, R(-), and S(+) flurbiprofen were approximately 9.0, 9.0, and 10.8 minutes. The method validation for R(-) and S (+) flurbiprofen in plasma and CSF met FDA requirements for accuracy, precision, recovery, linearity, stability, matrix effects, and selectivity.

Pharmacogenetic

Genomic DNA was extracted from peripheral blood leukocytes using the E.Z.N.A.™ SQ Blood DNA Kit. SNP genotyping analysis for CYP3A4*1G (rs2242480), CYP3A5*3 (rs776746), ABCB1 [1236C > T (rs1128503), 3435C > T (rs1045642), and 2677G > T/A (rs2032582)], ABCG2 [421C > A (rs2231142)], POR*28 (rs1057868), PXR (rs6785049 and rs3814055), and CAR (rs2307424) was performed using the ABI Prism® SNaPshot™ Multiplex Kit (Applied Biosystems). Amplification and extension were carried out on a Veriti® PCR System (Applied Biosystems). The resulting PCR products were purified using shrimp alkaline phosphatase (Fermentas Life Sciences) and ExoI (New England Biolabs). Single base extensions for the genetic polymorphisms were then performed with the ABI Prism® SNaPshot™ Multiplex Kit. Finally, the repurified products underwent capillary electrophoresis in 96-well plates using an ABI 3730XL Genetic Analyzer (Applied Biosystems). Details of the primers used are provided in Table S1.

Population Pharmacokinetic Analysis

Nonlinear mixed-effects modeling was performed using the first-order conditional estimation with extended least squares (FOCE-ELS) method, implemented in Phoenix NLME software (version 8.3; Certara, St. Louis, MO). Data analysis and visualization were conducted using Phoenix NLME software along with R software (version 4.1.0) and its packages.

Structural Model

This study plotted the concentration-time curves of R(-) and S(+) flurbiprofen in plasma and CSF after intravenous administration, allowing for preliminary assessment of the drug's distribution and elimination trends in the patients.

Subsequently, one-compartment and two-compartment models were used for further confirmation of the structural model. This study used the exponential model to describe the inter-individual variability in pharmacokinetic (PK) parameters. Intra-individual variation was evaluated using additive error model (I), proportional error model (II), and combined error model (III).

$$OBS_{ij} = PRED_{ij} + \varepsilon_{ij_1} \tag{1}$$

$$OBS_{ij} = PRED_{ij} + \left(1 + \varepsilon_{ij2}\right) \tag{2}$$

$$OBS_{ij} = PRED_{ij} + \left(1 + \varepsilon_{ij2}\right) + \varepsilon_{ij1} \tag{3}$$

OBS_{ij} and $PRED_{ij}$ represent the observed and predicted concentration values for the i-th patient at the j-th time point, respectively. ε_{ij1} and ε_{ij2} represent the additive random error and the proportional random error, respectively. The optimal structural model was determined based on the evaluation of the objective function value (equal to twice the negative log-likelihood [−2LL]) and visual inspection of standard goodness-of-fit plots.

Population Covariate Analysis

Potential covariates, including demographic factors (age, sex, body weight, height, and BMI) and genetic polymorphisms (PXR rs3814055 and rs1523127; POR rs1057868 and rs1135612; ABCB1 rs1045642 and rs4148738; CYP2C9 rs1057910, rs1799853, and rs182132442; UGT1A9 rs28898617), were evaluated for their influence on PK parameters. Continuous covariates (age, weight, height, and BMI) were incorporated using a power function after normalization to their median values, as specified in Equation I. Categorical covariates, including sex and genetic polymorphisms, were modeled using indicator variables within an exponential function (Equation II), with the reference category coded as 0 and other categories assigned values of 1 or higher. Prior to model building, a visual covariate-screening procedure was conducted using scatter plots for continuous variables and box plots for discrete and genetic variables. All candidate covariates were pre-screened for clinical and biological plausibility. Furthermore, correlation analyses were conducted to address multicollinearity, ensuring that highly correlated variables were not simultaneously included. Covariates showing a potential relationship with a PK parameter during the screening process were included in the model for further evaluation as significant covariates.

$$P_i = P \times \left(\frac{Cov}{Mean_{Cov}}\right)^{\theta_{Cov}} \tag{4}$$

$$P_i = P \times e^{\theta_{Cov} \times Cov} \tag{5}$$

Subsequently, the initially screened covariates were incorporated into the baseline model, and the stepwise module in NLME software was used for a second round of screening, primarily based on OFV values. In the forward inclusion process, each covariate was added to the model sequentially; if the addition of a covariate resulted in a decrease in OFV greater than 3.84, that covariate was included in the model. If the decrease did not exceed 3.84, the covariate was excluded. Each inclusion of a covariate formed a new model, and the remaining covariates were added to this new model. In the backward elimination process, if the removal of a covariate resulted in an increase in OFV greater than 6.63, that covariate was retained in the model; if the increase did not exceed 6.63, the covariate was eliminated. Each elimination formed a new model, and the process continued until the final model was obtained.

Model Evaluation and Validation

The final model was internally validated by observing diagnostic plots, which included the Conditional Weighted Residuals vs Population Predicted Values (CWRES-PRED), Conditional Weighted Residuals vs Time After Dose (CWRES-TAD), Observed vs Population Predicted Values (DV-PRED), and Observed vs Individual Predicted Values (DV-IPRED). Additionally, the internal validation of the final model included the Visual Predictive Check (VPC) and Bootstrap method. The VPC creates a new dataset that matches the sample size of the original dataset based on the

parameters and their distribution obtained from the final model. This process was repeated 1,000 times to compare the 5%, 50%, and 95% percentiles of the simulated concentrations with the observed concentrations. In the Bootstrap validation, a confidence interval for a parameter was constructed through multiple resampling with replacement from a subset of samples, while the entire sample remains unknown. This process was repeated 1,000 times to compare the median of the parameter estimates and the 95% confidence interval (CI) with the parameter values from the final model.

Results

Characteristics of the Included Patients

In this study, 70 patients participated in this study at Peking University People's Hospital from October 2019 to June 2020. Sixty-seven patients were ultimately included because three patients did not have detectable genotypes. Separate plasma and CSF samples of flurbiprofen were collected from each patient at different time points. The results of the eleven SNPs are shown in Table 1, of which CYP2C9 and UGT1A9 were not mutated and were therefore excluded from further analysis. Among all the loci, rs3814055 (PXR), rs1135612 (POR), rs1045642 (ABCB1), and rs4148738 (ABCB1) conform to the Hardy-Weinberg equilibrium except for the rs1523127 (PXR) and rs1057868 (POR).

Table 1 Characteristics of Patients Included in the Study (n=67)

	Number (%)	Mean (SD)	Median (range)
No. of patients (samples)	67 (100)		
Sex			
Male	10		
Female	57		
Age (year)		71 (49, 83)	70 (67, 75)
Height (m)		1.62 (1.4, 1.8)	1.61 (1.58, 1.64)
Weight (kg)		71 (47, 96)	70 (64, 78)
BMI ($kg \times m^{-2}$)		27.3 (18.4, 40.1)	27.1 (25.1, 29.4)
BSA (m^2)		2.6 (2.0, 3.2)	2.6 (2.5, 2.7)
Dose regimen (mg)			
100, QD, i.v.	67 (100)		
Genotype			
PXR			
rs3814055 (CC/CT/TT)	28/32/7		
rs1523127 (AA/CA/CC)	3/60/4		
POR			
rs1057868 (AA/GA/GG)	17/41/9		
rs1135612 (CC/CT/TT)	7/33/27		
ABCB1			
rs1045642 (AA/GA/GG)	12/40/15		
rs4148738 (AA/GA/GG)	15/37/15		

(*Continued*)

https://doi.org/10.2147/DDDT.S542722

Table 1 (Continued).

	Number (%)	Mean (SD)	Median (range)
CYP2C9			
rs1057910 (AA)	67 (100)		
rs1799853 (GG)	67 (100)		
rs182132442 (CC)	67 (100)		
rs1057910 (CC)	67 (100)		
UGT1A9			
rs28898617 (TT)	67 (100)		

Abbreviations: BMI, body mass index; SD, standard deviation; BSA, body surface area; i.v., intravenous.

Pharmacokinetic Study

The two-compartment structural model with exponential inter-individual variability terms provided adequate fits for both S(+) and R(-)-flurbiprofen concentrations in plasma and CSF based on goodness-of-fit plots and objective function value (OFV) comparisons. Plasma and CSF were conceptualized as the central and peripheral compartments, respectively (Figure S1).

Population Pharmacokinetic Analysis for S(+)-Flurbiprofen

The structural model for S(+)-flurbiprofen employed a combined additive and proportional error model. QQ plots of parameter η distributions demonstrated normal distribution patterns validating the exponential inter-individual variability model. Diagnostic plots of the structural model, including DV vs PRED and DV vs IPRED with close alignment along the identity line. The conditional weighted residuals (CWRES) vs PRED across predicted concentrations with >90% residuals within ±2 standard deviations.

During stepwise covariate modeling, BSA and ABCB1 genotype significantly reduced the −2 log-likelihood (−2LL) value (Δ-2LL > 3.84, $P < 0.05$) through forward inclusion. The ABCB1 genotype (rs1045642) was incorporated as a significant covariate influencing flurbiprofen clearance (CL), while BSA affected the volume of distribution. Backward elimination confirmed the necessity of ABCB1 genotype (rs1045642) retention whereas BSA elimination failed to demonstrate statistical significance. Table 2 summarizes the pharmacokinetic parameter estimates with inter-individual variability and residual error components.

Table 2 Pharmacokinetic Parameter Estimates and Bootstrap Results of Final PPK Model for S(+)-Flurbiprofen

Parameter Estimation		Bootstrap	
Parameter	**Estimate**	**Median**	**95% CI**
Fixed effects			
V_c, L	25.6	25.3	21.5–28.6
CL, L·h^{-1}	16.7	13.6	7.2–23.6
V_p, L	32.6	37.0	21.5–79.1
Q, L·h^{-1}	0.39	0.44	0.25–0.93
ABCB1 (rs1045642) on CL			
GA	−1.52	−0.96	−3.85 to −0.10
GG	0.19	0.29	−0.16 to 0.93

(*Continued*)

Table 2 (Continued).

Parameter Estimation		Bootstrap	
Parameter	**Estimate**	**Median**	**95% CI**
Interindividual variability (%)			
ωV_c	0.13	NA	NA
ωCL	0.16	NA	NA
ωV_P	0.25	NA	NA
ωQ	0.15	NA	NA
Random residual variability			
Plasma, additive error, σ	0.003	NA	NA
CSF, multiplicative error, σ	0.001	NA	NA

Abbreviations: 95% CI, 95% confidence interval; CL, apparent clearance; V_C, apparent volume of distribution in the central compartment; Q, intercompartment clearance; V_P, apparent volume of distribution in the peripheral compartment; ω, square root of interindividual variance for parameters; σ, residual variability; NA, not available.

The goodness-of-fit plots for the final model are shown in Figure 1, including DV versus IPRED, DV versus PRED, CWRES versus IVAR, and CWRES versus PRED, with no significant bias observed. Table 2 summarizes bootstrap validation results, confirming stability of final model parameters. Figure 2 displays time-stratified visual predictive checks (VPCs) and most of observed plasma and CSF concentrations within 5th–95th percentiles of model predictions, thereby validating robust predictive capacity across biological matrices.

Population Pharmacokinetic Analysis for R(-)-Flurbiprofen

The structural model of R-flurbiprofen adopts a proportional residual error model. The parameters η all follow a normal distribution, indicating that the exponential random effects model is suitable for this basic model in terms of individual differences. The DV vs PRED, DV vs IPRED, and CWRES vs PRED results of the structural model show no obvious bias.

The sequential addition of covariates, including BSA, BMI, POR (rs1057868) and POR (rs2868177) genotype, to the structural model significantly reduced the −2LL value of the model. Among these, BSA was found to significantly influence the central volume of distribution of flurbiprofen, while the POR (rs1057868) genotype significantly affected its clearance. Similarly, BMI and the POR (rs1057868) genotype were identified as significant factors affecting the peripheral volume of distribution of flurbiprofen. During the backward elimination process, the removal of BMI and POR (rs1057868) genotype covariates did not result in a significant increase in −2LL. In contrast, the exclusion of BSA and POR (rs1057868) genotype covariates caused a significant rise in −2LL. Consequently, BSA and S17 genotype covariates were retained in the final model. The pharmacokinetic parameters of the final model are detailed in Table 3.

The goodness-of-fit plots for the final model are presented in Figure 3, including DV versus IPRED, DV versus PRED, CWRES versus IVAR, and CWRES versus PRED, indicating that No significant bias was noted in these plots. Table 3 summarizes the bootstrap results for R-flurbiprofen, demonstrating that the parameters of the final model are consistent with the estimated parameters. The VPC plot indicates that the observed concentrations in plasma and CSF mostly fall within the 5% to 95% range of the corresponding predicted concentrations, confirming the model's strong predictive capability for R-flurbiprofen concentrations in both plasma and CSF.

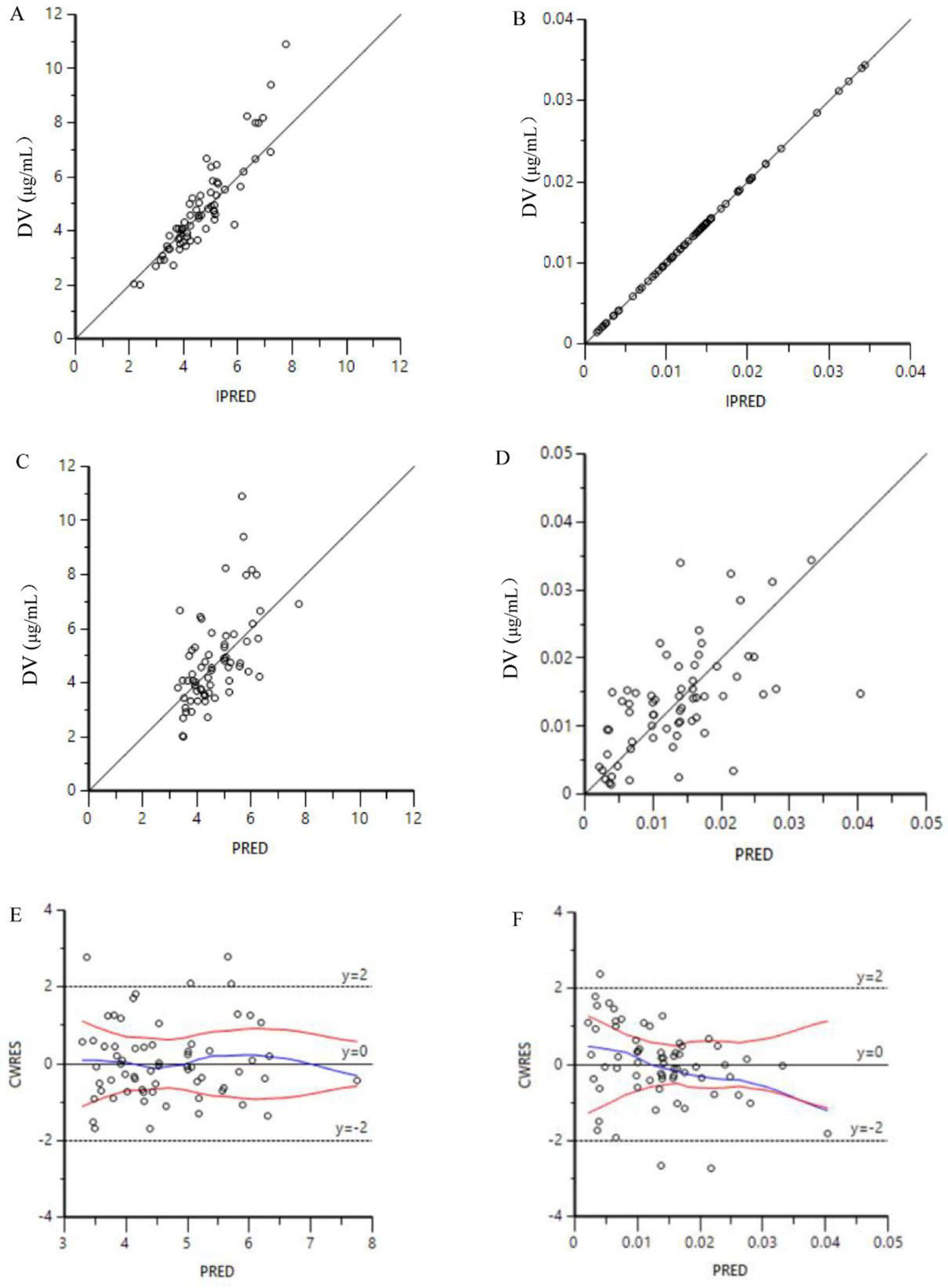

Figure 1 The goodness-of-fit plots for the final pharmacokinetic model for R(-)-flurbiprofen. (**A**), DV versus IPRED in the human plasma; (**B**), DV versus IPRED in the cerebrospinal fluid; (**C**), DV versus PRED in the human plasma; (**D**), DV versus PRED in the cerebrospinal fluid; (**E**), CWRES versus PRED in the human plasma; (**F**), CWRES versus PRED in the cerebrospinal fluid.

Abbreviations: PRED, population predictions; CWRES, conditional weighted residuals errors; IPRED, individual predictions; DV, observed concentrations.

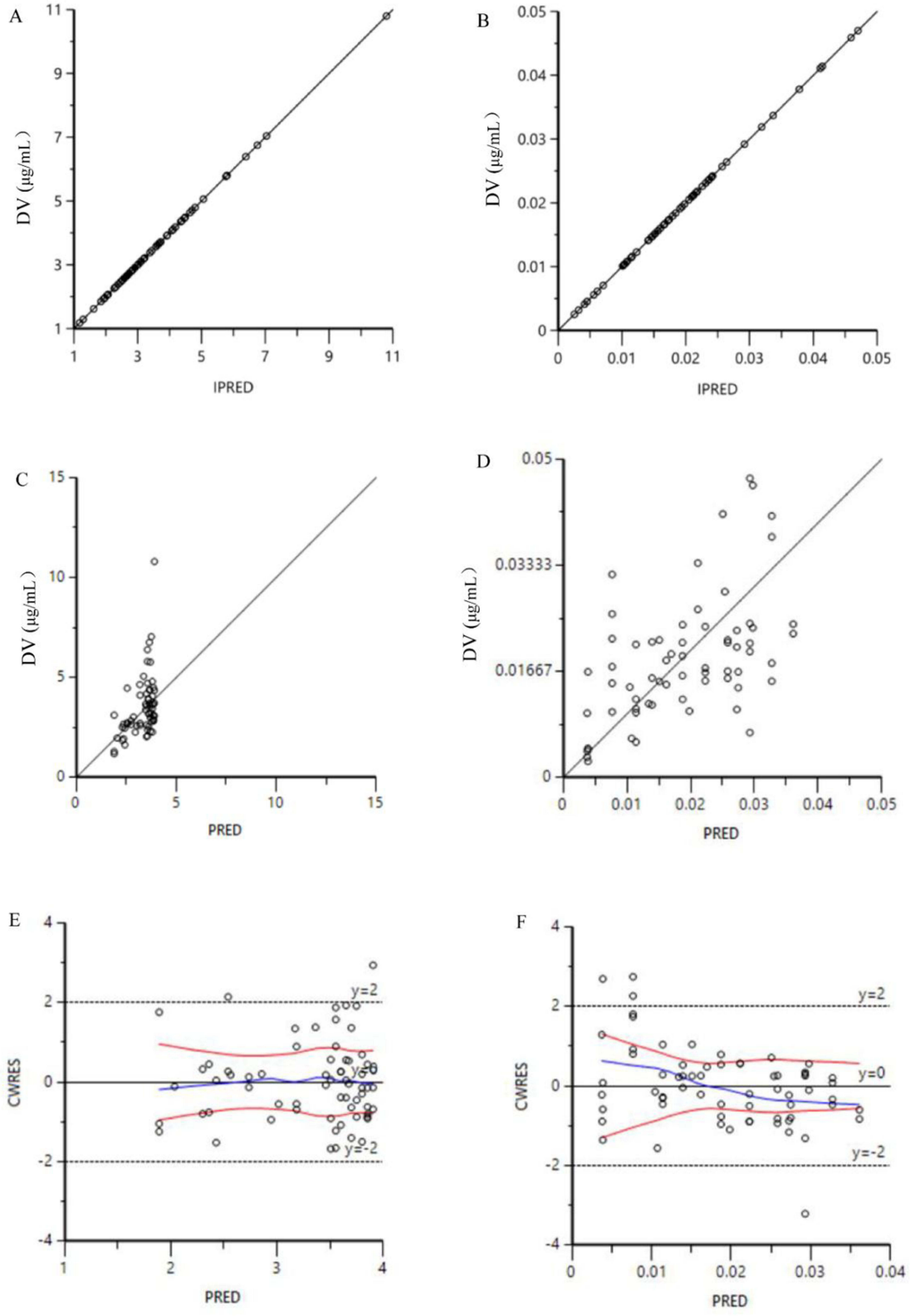

Figure 2 Visual predictive check (VPC) plots from the final model. (**A**), DV versus Time after dose of R(-)-flurbiprofen in the human plasma; (**B**), DV versus Time after dose of R(-)-flurbiprofen in the cerebrospinal fluid; (**C**), DV versus Time after dose of S(-)-flurbiprofen in the human plasma; (**D**), DV versus Time after dose of S(-)-flurbiprofen in the cerebrospinal fluid. The dots represent the observed concentrations, and the lines from top to bottom represent the 5th, 50th, and 95th percentiles of the predicted concentrations, respectively.

Abbreviation: DV, observed concentrations.

https://doi.org/10.2147/DDDT.S542722

Table 3 Pharmacokinetic Parameter Estimates and Bootstrap Results of Final PPK Model for R(-)-Flurbiprofen

Parameter Estimation		Bootstrap	
Parameter	**Estimate**	**Median**	**95% CI**
Fixed effects			
V_c, L	17.0	17.3	15.0–20.1
CL, L·h^{-1}	11.8	8.7	2.92–15.54
V_p, L	79.1	55.3	33.5–58.3
Q, L·h^{-1}	0.45	0.32	0.19 to 0.92
BSA on V_c	1.37	0.59	−0.07 to1.96
POR (rs1057868) on CL			
GA	−0.29	−0.15	−0.42 to −0.05
GG	−2.01	−1.42	−5.2 to −1.2
Interindividual variability (%)			
ωV_c	0.03	NA	NA
ωCL	0.12	NA	NA
ωV_p	0.22	NA	NA
ωQ	0.14	NA	NA
Random residual variability			
Plasma, additive error, σ	0.003	NA	NA
CSF, multiplicative error, σ	0.001	NA	NA

Abbreviations: 95% CI, 95% confidence interval; CL, apparent clearance; V_C, apparent volume of distribution in the central compartment; Q, intercompartment clearance; V_P, apparent volume of distribution in the peripheral compartment; ω, square root of interindividual variance for parameters; σ, residual variability; BSA, Body surface area; NA, not available.

Discussion

To the best of our knowledge, this study is the first to explore the pharmacokinetic and pharmacogenetic characterization of R(-) and S(+)-flurbiprofen in blood and CSF in patients and to establish a population pharmacokinetic model. It has been reported that the isomers of flurbiprofen show significant differences in the strength of their anti-inflammatory effects, with the S(+)-flurbiprofen inhibiting inflammation significantly more than the R-type of flurbiprofen.[11,13] Based on this characteristic, there have been literature reports on the development of S-flurbiprofen specifically for ocular drug delivery,[13] osteoarthritis[16,17] and Total Knee Arthroplasty.[18] R-flurbiprofen was considered a potential therapeutic candidate for Alzheimer's disease due to its ability to reduce lowered brain levels of Abeta.[19] This is mainly due to potential differences in pharmacological profiles resulting from the different three-dimensional structures of the different flurbiprofen isomers.[20,21] Distinct pharmacokinetic profiles may influence the neuropharmacological effects of flurbiprofen enantiomers, particularly through alterations in their apparent volume of distribution and clearance in the CSF. Therefore, elucidating the stereoselective pharmacokinetics of flurbiprofen isomers can provide a pharmacokinetic basis for their rational clinical application and support further development of enantiomer-specific formulations.

This study implemented a two-compartment model with plasma as the central compartment and CSF as the peripheral compartment, effectively characterizing enantiomer-specific pharmacokinetics. The estimated clearance rates for R(-)- and S(-)-flurbiprofen in the central compartment (11.76 vs 16.67 L/h, respectively) exceeded previously reported values

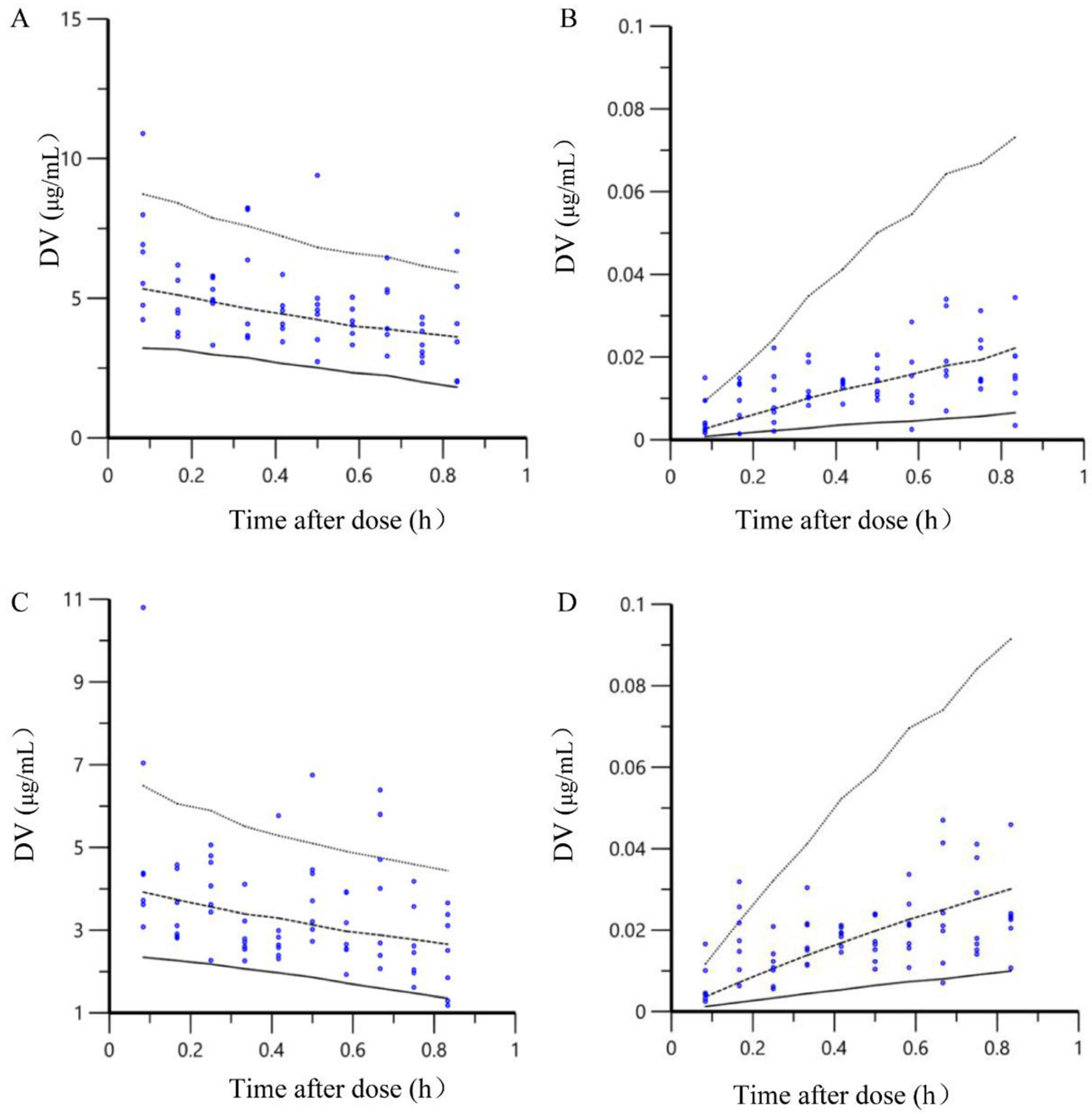

Figure 3 The goodness-of-fit plots for the final pharmacokinetic model for S(-)-flurbiprofen. (**A**), DV versus IPRED in the human plasma; (**B**), DV versus IPRED in the cerebrospinal fluid; (**C**), DV versus PRED in the human plasma; (**D**), DV versus PRED in the cerebrospinal fluid; E, CWRES versus PRED in the human plasma; F, CWRES versus PRED in the cerebrospinal fluid.

Abbreviations: PRED, population predictions; CWRES, conditional weighted residuals errors; IPRED, individual predictions; DV, observed concentrations.

for flurbiprofen.[22,23] These pharmacokinetic discrepancies likely originate from fundamental stereochemical differences between the measured enantiomers in our study and the racemic mixture analyzed in previous reports. Furthermore, we used a two-compartment model in this study, linking plasma and CSF, whereas previous studies usually used a one-compartment model, which may be responsible for the differences in pharmacokinetic parameters between the R(-)/S(+)-flurbiprofen and flurbiprofen. This result remains in need of further characterization as no pharmacokinetic literature data had been reported for similar isomers of flurbiprofen.

https://doi.org/10.2147/DDDT.S542722

Interestingly, we observed significant differences in the pharmacokinetics between R-flurbiprofen and S-flurbiprofen. Compared to R(-)-flurbiprofen, S(+)-flurbiprofen exhibits a larger apparent volume of distribution in the blood but a smaller apparent volume of distribution in the CSF. In terms of clearance, the clearance rate of S-flurbiprofen in the blood is higher than that of R-flurbiprofen, suggesting that S(+)-flurbiprofen may be metabolized more rapidly in the human body, resulting in a shorter residence time in the blood. These findings are similar with previous research reports.[15] Given that S(+)-flurbiprofen is metabolized more rapidly in the blood, developing S(+)-flurbiprofen as a standalone drug could be beneficial for achieving enhanced anti-inflammatory effects. In additional, the faster clearance of S(+)-flurbiprofen may render it particularly suitable for the management of acute inflammatory conditions, where rapid onset and short duration of action are often desirable. Specifically, we note that the larger distribution and slower clearance of the R-isomer in the CSF may support its potential application in neurological conditions such as Alzheimer's disease, where sustained central exposure is desirable. Future studies correlating CSF concentrations with clinical endpoints (eg, pain scores or biomarkers of neuroinflammation) are warranted to fully establish the exposure-response relationship.

Population pharmacokinetic modeling revealed that body surface area (BSA) significantly influences the apparent volume of distribution of R(-)-flurbiprofen, but not S(+)-flurbiprofen, while other demographic factors including age, weight, height, BMI, and gender showed no substantial impact on the pharmacokinetics of either enantiomer. A larger BSA is associated with a greater apparent volume of distribution for R-flurbiprofen, suggesting that the drug is distributed more widely throughout the body, resulting in relatively lower concentrations. This may be attributable to enantiomer-specific differences in tissue binding or partitioning mechanisms, potentially driven by variations in protein affinity or membrane transport between the R- and S-isomers. As a result, dose adjustments based on BSA could be particularly relevant for R-flurbiprofen to achieve effective therapeutic exposure, especially in patients with extreme body size. Furthermore, BSA may serve as a more robust indicator of metabolic mass than body weight alone, as it better reflects lean body mass and is less influenced by abnormal adipose tissue.

Flurbiprofen is primarily metabolized by the CYP2C9 gene, therefore, polymorphisms in the CYP2C9 gene may be a significant factor contributing to interindividual variability in flurbiprofen response.[7,24,25] The previous study reported that the CYP2C9 genotype is a significant predictor of flurbiprofen metabolism, explaining 59% of the variability in the area under the curve (AUC) of orally administered flurbiprofen. The AUC of flurbiprofen was significantly higher in individuals with the CYP2C9*1/*3 genotype, and the clearance of flurbiprofen was significantly lower compared to individuals with the *1/*1 genotype.[7] Although CYP2C9 genotyping was performed for all enrolled patients, the results revealed that all participants carried the wild-type genotype, thereby preventing further analysis of this variable. Previous studies have demonstrated that the frequency of the CYP2C9 wild-type genotype ranges from 77.27% to 94.4%, indicating that mutations at the CYP2C9 gene locus are relatively rare in the Chinese population.[26] Therefore, it is necessary to further expand the sample size in future studies to evaluate the impact of CYP2C9 gene polymorphisms on the pharmacokinetics of flurbiprofen isomers.

In this study, polymorphisms in the ABCB1 and POR genes were found to significantly affect the clearance of S(-) and R (-)- flurbiprofen, respectively. The PPK model revealed that the GA genotype of the ABCB1 gene inhibits the clearance of S-flurbiprofen, while the GG genotype increases its clearance rate, indicating that ABCB1 gene polymorphisms play a significant role in modulating drug metabolism. The ABCB1 gene encodes P-glycoprotein (P-gp), a critical drug transporter whose polymorphisms have been widely recognized to significantly influence drug absorption, distribution, metabolism, and excretion processes, particularly in drug transport across the intestine, blood-brain barrier, as well as the liver and kidneys.[27] This result is likely because the ABCB1 polymorphism (GA genotype) leads to increased distribution of S-flurbiprofen into the CSF, while in the liver and kidneys, reduced P-gp function results in slower excretion processes. Furthermore, the PPK model demonstrated that the GA and GG genotypes of the POR gene significantly inhibit the clearance of R-flurbiprofen compared to the AA genotype. Cytochrome P450 oxidoreductase (POR) plays a crucial role in the metabolism of drugs and steroids by supplying electrons to microsomal cytochrome P450 (CYP) enzymes.[28,29] It was hypothesized that the observed reduction in R-flurbiprofen clearance in subjects with POR GA or GG genotypes may be attributed to compromised electron transfer from POR to CYP450 enzymes in the liver, potentially suppressing oxidative metabolic capacity and consequently

delaying drug elimination. This evidence suggests that individualized use of flurbiprofen should take into account the genetic polymorphisms of both ABCB1 and POR.

The limitations of this study warrant careful consideration as they may impact the generalizability of the findings. Firstly, the relatively small sample size without external validation restricts the ability to draw definitive conclusions regarding the pharmacokinetic profiles of flurbiprofen across diverse patient populations. Future validation through multi-center collaborations or external datasets will be essential to confirm these findings and enhance the model's generalizability. Additionally, the absence of long-term follow-up assessments limits the understanding of the temporal dynamics of drug metabolism and clearance, potentially obscuring variations that may arise in chronic usage scenarios. Furthermore, the reliance on a single geographical cohort may introduce biases that do not reflect broader population characteristics, thereby affecting the applicability of the results. While genetic variability has been explored, the complexity of gene-environment interactions remains underrepresented, suggesting that further research integrating these dimensions is essential for a more comprehensive understanding of flurbiprofen pharmacokinetics. Additionally, due to medical ethics and humanitarian considerations, we were unable to collect CSF samples from the same patient multiple times; only one CSF sample could be obtained from each participant. This constraint limited our ability to characterize longitudinal pharmacokinetics and may have introduced additional inter-individual variability through the grouped sampling design. Consequently, we randomized patients into ten groups based on the timing of CSF sampling after drug administration, with an average of seven patients per group. The effect of CYP2C9 gene polymorphisms on the isomers of flurbiprofen could not be evaluated in this study, mainly due to the limited inclusion of samples and the failure to detect mutations at the gene locus. Therefore, it is imperative to further explore the effects of CYP2C9 gene polymorphisms on the pharmacokinetics of flurbiprofen isomers. It is noteworthy that the observed deviation from Hardy-Weinberg equilibrium for the POR (rs1523127) and PXR (rs1523127) SNP may be attributable to the limited sample size, which can amplify random fluctuations in genotype frequencies. Future studies with larger sample sizes are warranted to validate these findings and to obtain more precise estimates of the genetic effects.

Conclusion

This study established validated population pharmacokinetic models for both R(-) and S(-)- flurbiprofen using a structural two-compartment framework that accurately captured their stereoselective pharmacokinetic profiles. S (+)-flurbiprofen had a smaller volume of distribution and higher clearance than R(-)-flurbiprofen. ABCB1 gene polymorphism significantly affects S-flurbiprofen pharmacokinetics, while BSA and POR gene polymorphisms are key factors for R-flurbiprofen. These results offer valuable mechanistic insights into the enantiomer-specific pharmacokinetics of flurbiprofen, which may contribute to future research on dose optimization and support the development of tailored therapeutic strategies.

Data Sharing Statement

The research data are confidential but may be provided by the corresponding author for legitimate academic purposes upon approved request.

Ethical Approval Statement

This study was approved by Ethical Review Committee of Peking University People's Hospital (#2019PHB169-01) and registered as a clinical trial (ClinicalTrials.gov Identifier: NCT04128410). This study was conducted in accordance with the Declaration of Helsinki. All patient personal information was kept strictly confidential and was accessible only to authorized research personnel.

Disclosure

The authors report no conflicts of interest in this work.

References

1. Saleh F, Jackson TD, Ambrosini L, et al. Perioperative nonselective non-steroidal anti-inflammatory drugs are not associated with anastomotic leakage after colorectal surgery. *J Gastrointest Surg*. 2014;18(8):1398–1404. doi:10.1007/s11605-014-2486-4
2. Cata JP, Guerra CE, Chang GJ, Gottumukkala V, Joshi GP. Non-steroidal anti-inflammatory drugs in the oncological surgical population: beneficial or harmful? A systematic review of the literature. *British J Anaesth*. 2017;119(4):750–764.
3. Ahmadi M, Bekeschus S, Weltmann KD, von Woedtke T, Wende K. Non-steroidal anti-inflammatory drugs: recent advances in the use of synthetic COX-2 inhibitors. *RSC Med Chem*. 2022;13(5):471–496. doi:10.1039/D1MD00280E
4. Geng W, Hong W, Wang J, et al. Flurbiprofen axetil enhances analgesic effects of sufentanil and attenuates postoperative emergence agitation and systemic proinflammation in patients undergoing tangential excision surgery. *Media Inflamm*. 2015;2015(1):601083. doi:10.1155/2015/601083
5. Chen X, Chen P, Chen X, Huang M, Tang K, He Q. Efficacy and safety of parecoxib and flurbiprofen axetil for perioperative analgesia in children: a network meta-analysis. *Front Med*. 2023;10:1231570. doi:10.3389/fmed.2023.1231570
6. Huang L, Zheng X, Zhang Y, et al. Flurbiprofen axetil alleviates the effect of formalin-induced inflammatory pain on the cognitive function of rats with mild cognitive impairment through the AMPKα/NF-κB signaling pathway. *Ann Transl Med*. 2022;10(22):1210. doi:10.21037/atm-22-4997
7. Lee CR, Pieper JA, Frye RF, Hinderliter AL, Blaisdell JA, Goldstein JA. Differences in flurbiprofen pharmacokinetics between CYP2C9*1/*1, *1/*2, and *1/*3 genotypes. *Euro J Clin Pharmacol*. 2003;58(12):791–794. doi:10.1007/s00228-003-0574-6
8. Wang L, Bao SH, Pan PP, et al. Effect of CYP2C9 genetic polymorphism on the metabolism of flurbiprofen in vitro. *Drug Develop Indust Pharm*. 2015;41(8):1363–1367. doi:10.3109/03639045.2014.950274
9. Kumpulainen E, Välitalo P, Kokki M, et al. Plasma and cerebrospinal fluid pharmacokinetics of flurbiprofen in children. *British J Clin Pharmacol*. 2010;70(4):557–566. doi:10.1111/j.1365-2125.2010.03720.x
10. Zhang J, Zhang H, Zhao L, Gu J, Feng Y, An H. Population pharmacokinetic modeling of flurbiprofen, the active metabolite of flurbiprofen axetil, in Chinese patients with postoperative pain. *J Pain Res*. 2018;11:3061–3070. doi:10.2147/JPR.S176475
11. Uwai Y, Matsumoto M, Kawasaki T, Nabekura T. Enantioselective effect of flurbiprofen on lithium disposition in rats. *Pharmacology*. 2017;99(5–6):236–239. doi:10.1159/000455917
12. Luo J, Yuan L, Yang L, Wang H, Zhou M. Chiral S-flurbiprofen axetil-loaded lipid microspheres for improved analgesic effects: preparation, characterization, and preclinical evaluation. *J Drug Delivery Sci Technol*. 2024;92:105407. doi:10.1016/j.jddst.2024.105407
13. Ma Z, Wang Y, He H, Liu T, Jiang Q, Hou X. Advancing ophthalmic delivery of flurbiprofen via synergistic chiral resolution and ion-pairing strategies. *Asian J Pharmace Sci*. 2024;19(3):100928. doi:10.1016/j.ajps.2024.100928
14. Wong LR, Ho PC. Role of serum albumin as a nanoparticulate carrier for nose-to-brain delivery of R-flurbiprofen: implications for the treatment of Alzheimer's disease. *J Pharma Pharmacol*. 2018;70(1):59–69. doi:10.1111/jphp.12836
15. Yao H, Luo X, Zhang H, An H, Feng W, Feng Y. The comparison of plasma and cerebrospinal fluid R(-)- and S(+)-flurbiprofen concentration after intravenous injection of flurbiprofen axetil in human subjects. *Front Pharmacol*. 2021;12:646196. doi:10.3389/fphar.2021.646196
16. Yataba I, Otsuka N, Matsushita I, Matsumoto H, Hoshino Y. The long-term safety of s-flurbiprofen plaster for osteoarthritis patients: an open-label, 52-week study. *Clin Drug Invest*. 2016;36(8):673–682. doi:10.1007/s40261-016-0412-0
17. Yataba I, Otsuka N, Matsushita I, Matsumoto H, Hoshino Y. The efficacy and safety of S-flurbiprofen plaster in the treatment of knee osteoarthritis: a Phase II, randomized, double-blind, placebo-controlled, dose-finding study. *J Pain Res*. 2017;10:867–880. doi:10.2147/JPR.S131779
18. Tsuji M, Kobayashi N, Yukizawa Y, Oishi T, Takagawa S, Inaba Y. Effect of flurbiprofen and S-flurbiprofen patches on multimodal pain management after total knee arthroplasty: a prospective randomized controlled trial. *J Arthroplasty*. 2020;35(8):2033–2038. doi:10.1016/j.arth.2020.04.006
19. Geerts H. Drug evaluation: (R)-flurbiprofen–an enantiomer of flurbiprofen for the treatment of Alzheimer's disease. *IDrugs*. 2007;10(2):121–133.
20. Radwan MA, Aboul-Enein HY. In vitro release and stereoselective disposition of flurbiprofen loaded to poly(D,L-lactide- co-glycolide) nanoparticles in rats. *Chirality*. 2004;16(2):119–125. doi:10.1002/chir.10314
21. Yataba I, Otsuka N, Matsushita I, et al. Plasma pharmacokinetics and synovial concentrations of S-flurbiprofen plaster in humans. *Euro J Clin Pharmacol*. 2016;72(1):53–59. doi:10.1007/s00228-015-1960-6
22. Suri A, Grundy BL, Derendorf H. Pharmacokinetics and pharmacodynamics of enantiomers of ibuprofen and flurbiprofen after oral administration. *Inter J Clin Pharmacol Therap*. 1997;35(1):1–8.
23. Qayyum A, Najmi MH, Farooqi ZU. Determination of pharmacokinetics of flurbiprofen in Pakistani population using modified HPLC method. *J Chromatographic Sci*. 2011;49(2):108–113. doi:10.1093/chrsci/49.2.108
24. Wang B, Wang J, Huang SQ, Su HH, Zhou SF. Genetic polymorphism of the human cytochrome P450 2C9 gene and its clinical significance. *Curr Drug Metabol*. 2009;10(7):781–834. doi:10.2174/138920009789895480
25. Whang SS, Cho CK, Jung EH, et al. Physiologically based pharmacokinetic (PBPK) modeling of flurbiprofen in different CYP2C9 genotypes. *Arch Pharmacal Res*. 2022;45(8):584–595. doi:10.1007/s12272-022-01403-4
26. Zhang J, Chen Z, Chen C. Impact of CYP2C9, VKORC1 and CYP4F2 genetic polymorphisms on maintenance warfarin dosage in Han-Chinese patients: a systematic review and meta-analysis. *Meta Gene*. 2016;9:197–209. doi:10.1016/j.mgene.2016.07.002
27. Wolking S, Schaeffeler E, Lerche H, Schwab M, Nies AT. Impact of genetic polymorphisms of ABCB1 (MDR1, P-glycoprotein) on drug disposition and potential clinical implications: update of the literature. *Clin Pharmacok*. 2015;54(7):709–735. doi:10.1007/s40262-015-0267-1
28. Gong L, Zhang CM, Lv JF, Zhou HH, Fan L. Polymorphisms in cytochrome P450 oxidoreductase and its effect on drug metabolism and efficacy. *Pharmacogen Genomics*. 2017;27(9):337–346. doi:10.1097/FPC.0000000000000297
29. Naldi GAR, Minari AB, Pereira TDM, et al. CYP3A5 and POR gene polymorphisms as predictors of infection and graft rejection in post-liver transplant patients treated with tacrolimus - a cohort study. *Pharmacogen J*. 2025;25(2):4. doi:10.1038/s41397-025-00363-4